

# Wavefront control of UV narrow bandpass filters prepared by plasma ion-assisted deposition

Jue Wang<sup>\*</sup>, Robert L. Maier, Horst Schreiber  
Corning Tropol Corporation, 60 O'Connor Road, Fairport, NY, USA 14450-1376

## ABSTRACT

Metal oxide layers produced by plasma ion-assisted deposition are extensively used for complex optical coatings due to the availability of materials, the high packing density of films, and the smooth surfaces. Stringent optical surface figure specifications necessary for both laser optics and precision optics require film stress to be well controlled and surface deformation to be corrected or compensated. In this paper, SiO<sub>2</sub> based single cavity UV narrow bandpass filters were prepared by plasma ion-assisted deposition. The correlation between film stress, refractive index, deposition parameters, and post deposition annealing was established. The film stress was calculated based on interferometric surface deformation. The refractive index and film thickness were determined by means of variable angle spectroscopic ellipsometry. The center wavelength of the filters was obtained through spectral transmission measurement. The results suggest that the wavefront distortion of the multilayer coatings is dominated by the compressive stress of the SiO<sub>2</sub> layers, and can be controlled and corrected by the amount of plasma ion momentum transfer, substrate temperature, post deposition annealing, and stress compensation via backside SiO<sub>2</sub> coating. Based on the understanding of the mechanical and optical properties, the wavefront correction technique enables us to satisfy stringent surface figure specifications.

**Keywords:** UV narrow bandpass filter, plasma ion-assisted deposition, mechanical stress, optical properties, wavefront correction

## 1. INTRODUCTION

The increasing demand for optical elements used in precision optics and laser optics for UV applications requires multilayer coatings with low loss, long durability and minimum surface deformation. It is well known that films deposited by conventional methods have low packing density and absorb environmental moisture, leading to variations in optical performance.<sup>1</sup> With advanced deposition techniques, such as ion assisted deposition (IAD), plasma ion-assisted deposition (PIAD), ion-beam-assisted deposition (IBAD), film packing density can be improved significantly.<sup>2-4</sup> Smooth, dense coatings exhibiting low scatter and environmental stability can be achieved. However, two concerns remain. Over bombardment of plasma ions may generate dissociation of depositing materials. Also, the increased packing density may cause high mechanical stress. The former introduces absorption, typically in the UV spectral region, whereas the later alters the wavefront of optical elements as a result of surface deformation. The composition dissociation of metal oxide layers has been eliminated by means of reactive PIAD. The surface wavefront control depends upon understanding the correlations between film mechanical properties, optical properties, and deposition parameters.

Mechanical stress of metal oxide films is a property sensitive to the coating process. Tensile stress is expected for high refractive index metal oxide layers deposited by PIAD, because of the grain boundary effect of the crystalline dielectric films. For the low refractive index layers, SiO<sub>2</sub> is the most frequently used material suitable for PIAD. Multilayer metal oxide coatings produced by PIAD show high

---

<sup>\*</sup> [wangj3@corning.com](mailto:wangj3@corning.com) phone 1 585 388-3500; fax 1585 388-6332

compressive stress. Since multilayer coatings comprise approximately equal numbers of high refractive index and low refractive index layers, it is reasonable to assume that the net high compressive stress is dominated by low refractive index SiO<sub>2</sub> layers. As a result, the SiO<sub>2</sub> layers play a critical role for surface wavefront control of UV optical components.

As an aid to understanding and controlling stringent wavefront requirements, UV narrowband pass filters were deposited by PIAD to study the relationships among mechanical and optical properties, as well as the influence of deposition conditions and post treatment. Various wavefront control approaches were considered, including the amount of plasma ion momentum transfer, substrate temperature during deposition, post deposition annealing, and backside coating for stress compensation.

## 2. EXPERIMENTAL

The SiO<sub>2</sub>/Ta<sub>2</sub>O<sub>5</sub> based single cavity narrow bandpass filters were deposited on high purity fused silica (HPSF) substrates by PIAD. The diameter and thickness of the double side polished HPSF substrates were 40mm and 2.5mm, respectively. Prior to film deposition, the substrates were thermally treated to remove any residual stress carried over from optical surfacing and/or edging. The wavefront of the substrates was less than 0.04 fringes at the measured wavelength of 870nm in all cases.

Post deposition annealing was done at temperatures ranging from 120°C to 300°C. A slow annealing process was employed, in which the filter was annealed overnight (~10 hours) at a predefined temperature, with a few °C/min ramp rate for heating and cooling. The selection of the annealing time and slow cooling rate helps insure stabilization of the mechanical and optical properties.

The mechanical and optical properties of both single layers and narrow bandpass filters were evaluated under various deposition conditions, including plasma ion momentum transfer and substrate temperature during deposition. The changes to physical thickness and refractive index of the single layers were modeled by variable angle spectroscopic ellipsometer measurements for increased sensitivity.<sup>5,6</sup>

The center wavelength (CWL) of the NBF was determined through transmission measurement via a Perkin Elmer Lambda 19 spectrophotometer. The stress was calculated based on the substrate surface deformation measured by SCL 870 interferometer at a wavelength of 870nm. The short coherence length of the instrument enables one to distinguish one surface from the other.

## 3. RESULTS AND DISCUSSION

### 3.1 Stress simulation

Stress induced surface deformation, as a result of the coating process, can be determined by measuring surface figure both before and after coating. The change between the two measurements can be used to determine coating induced stress. If the thickness  $d_s$  of a spherical substrate is large compared with the thickness  $d_f$  of the deposited film, the total stress of a single layer can be calculated by a modification to Stoney's equation<sup>7,8</sup>

$$\sigma_s = \frac{2E_s}{3(1-\nu_s)} \left(\frac{d_s}{D}\right)^2 \frac{\lambda}{d_f} \Delta f \quad (1)$$

where  $E_s$  and  $\nu_s$  are Young's modulus and Poisson's ratio for the substrate.  $\lambda$  is the wavelength used for the wavefront measurement over a clear aperture with a diameter  $D$ .  $\Delta f$  is the net fringe change of the substrate surface deformation after coating. Conventionally, the positive sign represents tensile stress,

whereas the negative sign indicates compressive stress, corresponding to a concave and a convex surface deformation, respectively.

According to Eq. (1), a properly selected coating witness plate can be used to monitor mechanical properties of the optical elements if deposited with the same coating design. For the wavefront control of large UV optical components, there is a need to understand the correlation between the optical and mechanical properties. Since the center wavelength of a high order single cavity NBF is very sensitive to coating material properties, deposition conditions, and post treatment,<sup>8-10</sup> a UV NBF was designed to simulate the mechanical stress evolution of the actual UV components under various experimental conditions.

Fig. 1 shows the measured transmittance spectrum of a SiO<sub>2</sub>/Ta<sub>2</sub>O<sub>5</sub> multilayer UV NBF deposited on HPFS substrate by PIAD. The NBF contains 23 alternate Q/H layers. The center wavelength is at 386nm with a full width at half maximum (FWHM) of 0.7nm. The surface deformation resulted in 2.190 fringes of power at the measured wavelength of 870nm. The surface specification for the component was less than 0.04 fringes at 870nm, corresponding to 0.05 fringes at 633nm, for both the uncoated and the coated optics. According to Eq.(1), the calculated stress of the NBF is -230MPa, where the negative sign represents a compressive stress. Table 1 summarizes the parameters of the NBF.

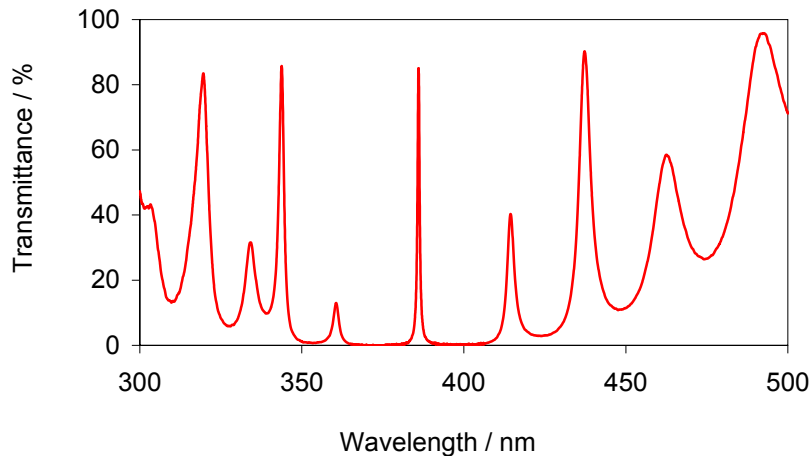


Fig. 1 Transmission spectrum of the UV NBF

Table 1 Description of the UV NBF

Sub	D (mm)	d <sub>s</sub> (mm)	Layer #	σ (MPa)	d <sub>f</sub> (nm)	f (fr.) at 870nm	f <sub>spec</sub> (fr.) at 870nm
HPFS	36.0	2.5	23	-230	2253	2.190	0.04

### 3.2 Effect of post deposition annealing

For metal oxide UV multilayer optical interference filters, post deposition annealing is a common technique for stabilizing and/or adjusting the CWL, and transmission or reflection spectra. Post deposition annealing reduces the stress of UV NBF.<sup>8</sup> As a result, the surface deformation can be relaxed to some degree. Fig. 2 shows the surface wavefront as well as the CWL shift of the UV NBF as a result of post annealing. The increased annealing temperature results in the reduction of the wavefront distortion, whereas a reverse trend

is observed for the CWL shift, i.e., the CWL of the annealed NBF is a few nanometers longer than the as-deposited filter.

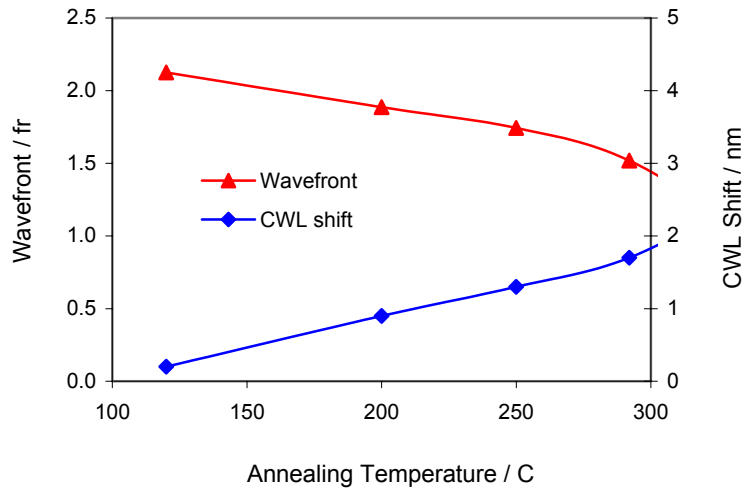


Fig. 2 Surface wavefront and CWL shift of the UV NBF as a function of post deposition annealing

The evaluation of individual coating materials enables one to precisely control the optical and mechanical properties of the UV NBF. Single layers of  $\text{SiO}_2$  and  $\text{Ta}_2\text{O}_5$  were deposited using the same PIAD parameters as for the UV NBS. Table 2 lists the stress values of  $\text{SiO}_2$  and  $\text{Ta}_2\text{O}_5$  single layers. As can be seen, the  $\text{SiO}_2$  layer has high compressive stress, whereas the  $\text{Ta}_2\text{O}_5$  shows tensile stress. The amount of stress of the  $\text{SiO}_2$  is about one order of magnitude higher than that of  $\text{Ta}_2\text{O}_5$ . The result suggests that the  $\text{SiO}_2$  layers play a dominated role of the net high compressive stress of the UV NBF.

Table 2 Stress of single layer of  $\text{SiO}_2$  and  $\text{Ta}_2\text{O}_5$

Single layer	$\sigma$ (MPa)	d (nm)
$\text{SiO}_2$	-244	997
$\text{Ta}_2\text{O}_5$	24	1004

Ellipsometric data taken around the quasi-Brewster angle of the single layers was acquired at various wavelengths prior to and after annealing at  $300^\circ\text{C}$ . The highly sensitive measurement of phase change around the quasi-Brewster angle enables us to monitor slight changes of film properties after annealing.<sup>6</sup> Fig. 3 depicts the refractive indices of the  $\text{SiO}_2$  single layer derived from the ellipsometric measurement prior to and after  $300^\circ\text{C}$  annealing.

After annealing at  $300^\circ\text{C}$ , the refractive index drops 0.18%, corresponding to 0.54% increase of porosity. The ellipsometric modeling also suggests an increased physical thickness of 3.6nm. The total optical thickness increase of 0.18% as a result of  $300^\circ\text{C}$  annealing of the  $\text{SiO}_2$  single layer, is consistent with the measured CWL upward shift of the UV NBF annealed at the same temperature, as shown in Fig. 2. For films deposited by magnetron and ion-beam sputtering, some similar observations of increased porosity have been reported for single layers of  $\text{ZrO}_2$ ,  $\text{Ta}_2\text{O}_5$  and  $\text{SiO}_2$  after annealing.<sup>10-12</sup>

In addition, the ellipsometric modeling suggests that the surface RMS of the SiO<sub>2</sub> single layer increased to 1.76nm from 1.10nm after the annealing. The increased RMS is an indication of stress relaxation due to the post-deposition annealing, which has been further confirmed by AFM measurement.<sup>6</sup>

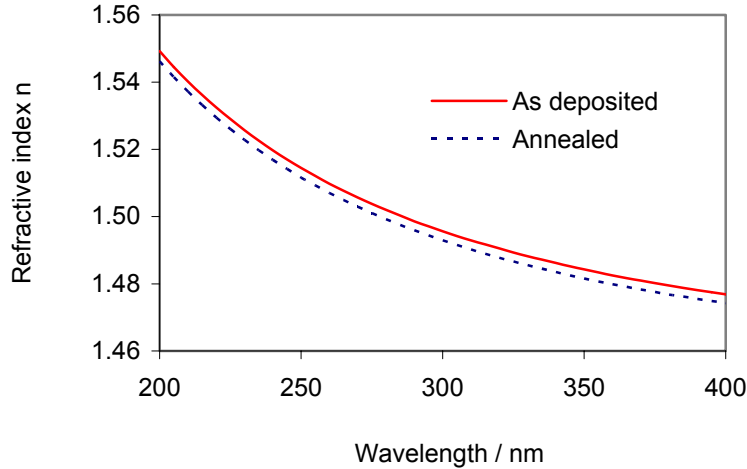


Fig. 3 Refractive indices of the SiO<sub>2</sub> layer prior to and after post deposition annealing

### 3.3 Effect of plasma momentum transfer

As a coating process sensitive property, mechanical stress of metal oxide films has been an interesting research topic for UV optics.<sup>13</sup> In general, metal oxide films prepared by electron-beam reactive evaporation with substrate temperatures in the range 20°C to 300°C, may exhibit tensile or compressive stress. On the other hand, films deposited by energetic technologies, such as PIAD, produce compressive stress in most cases. One can vary the stress value of oxide films by adjusting the conditions of kinetic growth as well as by modifying the bombarding parameters. The compressive stress appears to be momentum rather than energy driven.<sup>14</sup> Instead of using several process parameters such as bias voltage and deposition rate, the momentum transfer per deposited atom P is selected as a combined parameter which dominates film stress. The P can be described by:

$$P = \frac{J_i}{R} \kappa \sqrt{2m_i e V_b} \quad (2)$$

where  $V_b$  is the bias voltage,  $J_i$  and  $m_i$  are the plasma ion flux in ion/(cm<sup>2</sup>sec) and mass in a.u., respectively. R is the deposition rate in nm/sec. e is the electron charge and k is a unit conversion factor.

Fig. 4 shows the compress stress of 500nm SiO<sub>2</sub> single layers as a function of plasma ion momentum transfer per deposited atom at a substrate temperature of 120°C. Accordingly, the stress of the SiO<sub>2</sub> film  $\sigma$  can be described in a unit of MPa by:

$$\sigma = \frac{1}{18} d^{1/8} e^{(P/58)} \quad (3)$$

where  $d$  is the  $\text{SiO}_2$  layer thickness in nm,  $P$  is the plasma momentum transfer per deposited atom described in Eq.(2). As can be seen in the figure, the  $\text{SiO}_2$  layer has high compressive stress ranging from 100 MPa up to 400 MPa. The result confirms that  $\text{SiO}_2$  film stress can be adjusted by varying the amount of plasma momentum transfer. In addition, the film stress is also a function of the film thickness.

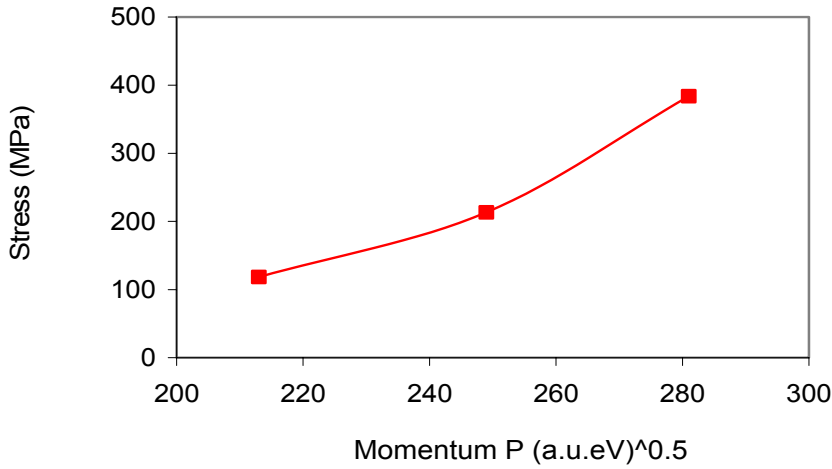


Fig.4 Compressive stress of a 500nm  $\text{SiO}_2$  single layer as a function of plasma ion momentum transfer per deposited atom

Fig. 5 shows the refractive indices of  $\text{SiO}_2$  single layers deposited with various amounts of plasma momentum transfer, 213 (a.u. eV)<sup>0.5</sup>, 249 (a.u. eV)<sup>0.5</sup> and 281 (a.u. eV)<sup>0.5</sup>, labeled as P<sub>a</sub>, P<sub>b</sub> and P<sub>c</sub>, respectively. The refractive index of the HPFS substrate is also plotted in the same figure for comparison. With low plasma bombardment (P<sub>c</sub>) the refractive index of the  $\text{SiO}_2$  film is lower than the substrate. With medium plasma bombardment (P<sub>b</sub>) the refractive index of the  $\text{SiO}_2$  film is just slightly higher than the substrate. Further increasing the plasma momentum transfer produces a refractive index of the  $\text{SiO}_2$  film even higher than the substrate. Comparing the  $\text{SiO}_2$  single layer results shown in Fig. 4 and Fig. 5 it is clear that the optical properties and mechanical properties are correlated, i.e., high stress corresponds to high refractive index. The result is also consistent with the stress reduction and the CWL upward shift after post deposition annealing of the UV NBF shown in Fig. 2.

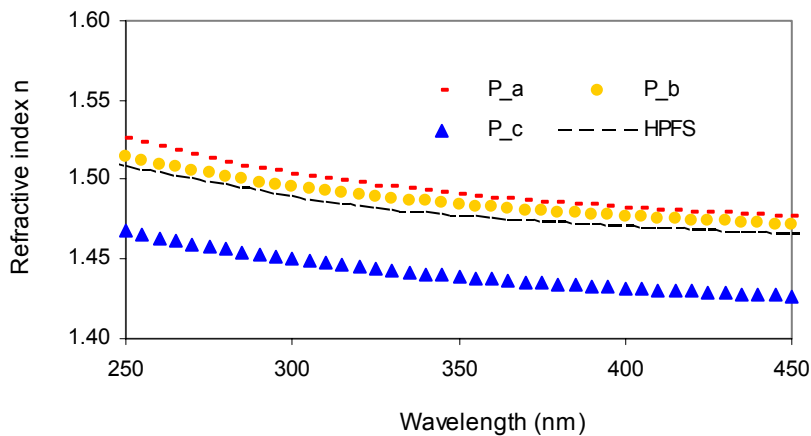


Fig. 5 Refractive index of  $\text{SiO}_2$  single layers for various plasma ion momentum transfers during deposition, compared to HPFS substrate

### 3.4 Effect of substrate temperature

The plasma ion momentum transfer per deposited atom is a very important parameter for PIAD process control. As described in Eq.(1), the P comprises many deposition parameters, including bias voltage, deposition rate, plasma ion flux and mass. Substrate temperature during deposition may be another important parameter if considering mechanical stress of coatings. As discussed in the subsection 3.3, plasma ion momentum transfer determines the optical properties as well as the intrinsic stress of the film. However, film stress relaxation occurs as a result of post deposition annealing, suggesting varying substrate temperatures during deposition may enable one to alter film stress as well. Table 3 lists the amount of stress for the filters deposited at different substrate temperatures. Indeed, filters deposited at relatively high substrate temperature have low compressive stress. The result is comparable to that obtained from the post deposition annealing, as discussed in the subsection 3.1

Table 3 Deposition temperature effect on the stress of NBF

Sub temperature (°C)	120	240	280
$\sigma$ of NBF (MPa)	-230	-125	-123

### 3.5 Backside SiO<sub>2</sub> coating

Several approaches have been evaluated for adjusting the surface wavefront of the UV NBF, including post deposition annealing, plasma ion momentum transfer and substrate temperature during deposition. To reach the target of surface figure specification listed in Table 1 (0.04 fr. at 870nm or 0.05 fr at 633nm), a precise wavefront correction technique is required.

Since SiO<sub>2</sub> based UV multilayer coatings have high compressive stress, stress compensation may be accomplished by a predetermined thickness of SiO<sub>2</sub> deposited on the backside of the optic according to Eq.(3). Fig. 6 shows the calculated SiO<sub>2</sub> layer thicknesses vs different values of P, necessary for correcting a NBF deposited at 280°C with a surface deformation of 1.17 fringes at wavelength 870nm. As can be seen, less film thickness is required for back side correction, when larger values of P are applied during SiO<sub>2</sub> film deposition. To experimentally evaluate the calculation, 605nm SiO<sub>2</sub> was deposited on the backside of the element at a momentum transfer of P<sub>c</sub>. The wavefront measured on the front surface of the element was reduced to 0.114 fringes from 1.170 fringes. The results listed in Table 4 suggest that depositing 91% of calculated amount of SiO<sub>2</sub> corrected 90% of the surface deformation. The wavefront correction thickness for the backside SiO<sub>2</sub> coating is calculated at 573nm/fr. The final corrected wavefront is expected to be 0.009 fr, if the calculated 665nm thickness of SiO<sub>2</sub> is deposited, which is less than 0.04 fr at 870nm specification.

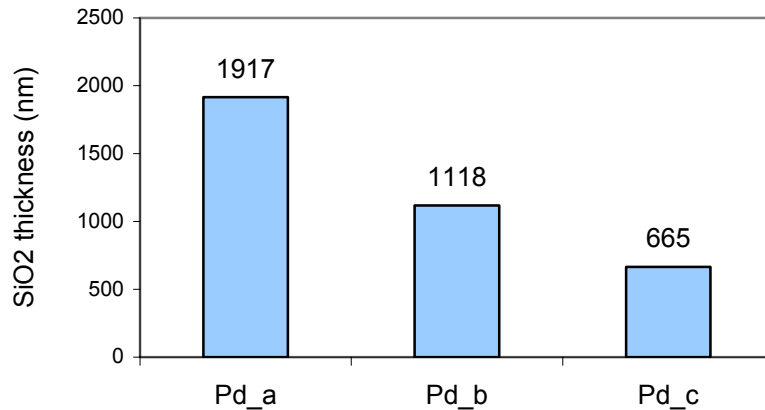


Fig. 6 Calculated backside SiO<sub>2</sub> thickness at various plasma momentum transfers

Table 4 Example of surface correction

Backside SiO <sub>2</sub> (nm)	665 (calculated)	605 (actual deposited)
Front surface deformation (fr. at 870nm)	1.170 (Uncorrected NBF)	0.114 (corrected)

#### 4. CONCLUSIONS

SiO<sub>2</sub>/Ta<sub>2</sub>O<sub>5</sub> multilayer UV narrow bandpass filters were deposited on HPFS substrates by PIAD. The optimized PIAD process led to a densified multilayer coating with a stabilized built-in compressive stress. Single layer tests indicated that the stress of the NBF was dominated by the SiO<sub>2</sub> layers, which were 10x higher than the corresponding Ta<sub>2</sub>O<sub>5</sub> layers. The stress of SiO<sub>2</sub> layers is compressive, whereas the Ta<sub>2</sub>O<sub>5</sub> layers are tensile. The wavefront distortion of the NBF was partially eliminated by means of post deposition annealing. Simultaneously, a CWL upward shift was observed and correlated to the film stress relaxation. The results were confirmed by advanced ellipsometric modeling of the annealed single layers. The stress relaxation of the films results in a reduced refractive index and an increased physical thickness. The high compressive stress of SiO<sub>2</sub> layers can be altered by varying the amount of plasma ion momentum transfer during film deposition. Increased plasma ion bombardment raises the refractive index of the SiO<sub>2</sub> films due to an increased film packing density. In addition, the stress of the NBF was reduced by increasing substrate temperature during deposition. The understanding of mechanical and optical properties of the UV narrow bandpass filters enables us to precisely determine the amount of backside SiO<sub>2</sub> coating necessary to meet the surface requirement of less than 0.05 fringes of power at 633nm. The wavefront correction technology also enables us to use small witness plates to simulate the stress behaviors of large optics and precisely correct the stress related surface deformations.

#### REFERENCES

1. Karl Gunther, *Applied Optics* Vol.23 (1984) pp3806-3816
2. H. Takashashi, "Temperature stability of thin-film narrow-bandpass filter produced by ion-assisted deposition", *Applied Optics* **34**, 667-675(1995)
3. A. Zöller, R. Götzelmann, K. Matl, D. Cushing, "Temperature-stable bandpass filters deposited with plasma ion-assisted deposition", *Applied Optics* **35**, 5609-5612(1996)

4. R. Y. Tsai, C. S. Chang, C. W. Chu, T. Chen, F. Dai, S. Yan, A. Chang, "Thermally stable narrow-bandpass filter prepared by reactive ion-assisted sputtering", *Applied Optics* **40**, 1593-1598(2001)
5. J. N. Hilfiker, C. L. Bungay, R. A. Synowicki, T. E. Tiwald, C. M. Herzinger, B. John, G. K. Pribil, J. A. Woollam, "Progress in spectroscopic ellipsometry: Applications from vacuum ultraviolet to infrared", *J. Vac. Sci. Tech. A* **21**, 1103-1108(2003).
6. J. Wang, R. L. Maier, "Quasi-Brewster angle technique for evaluation the quality of optical surfaces", *Proc. SPIE* **5375**, 1286-1294(2004).
7. D. L. Smith (ed.), *Thin-film deposition principles & practice*, Charter 5, McGraw-Hill, Inc. (1995)
8. J. Wang, R. L. Maier, "Correlation between mechanical stress and optical properties of SiO<sub>2</sub>/Ta<sub>2</sub>O<sub>5</sub> multilayer UV narrow-bandpass filters deposited by plasma ion-assisted deposition", *Proc. SPIE* **5870**, 587000E1-9(2005).
9. S. H. Kim, C. K. Hwangbo, "Derivation of the center-wavelength shift of narrow bandpass filters under temperature change", *Optics Express* **12**, 5636-5639(2004)
10. J. T. Brown, "Center wavelength shift dependence on substrate coefficient of thermal expansion for optical thin-film interference filters deposited by ion-beam sputtering", *Applied Optics* **43**, 4506-4511(2004)
11. Y. Z. Hu, S. P. Tay, "Characterization of high-K dielectric ZrO<sub>2</sub> films annealed by rapid thermal process," *J. Vac. Sci. Technol. B* **19**, 1706-1714(2001)
12. S. M. Lee, A. Dummer, C. Montcalm, "Annealing effects on the properties of optical filters," in *Proceedings of the Society of Vacuum Coaters 45<sup>th</sup> Annual Technical Conference*, 220-223(2002)
13. R. Thielsch, A. Gatto, N. Kaiser, "Mechanical stress and thermal-elastic properties of oxide coating for use in the deep-ultraviolet spectral region", *Applied Optics* **41**, 3211-3217(2002)
14. H. Windischmann, "Intrinsic stress in sputtered thin films", *J. Vac. Sci. Technol. A* **9**(4), 2431-2436(1991)